FOR THE RECORD

C-terminal juxtamembrane region of full-length M2 protein forms a membrane surface associated amphipathic helix

Shenstone Huang,[1] Bryan Green,[1] Megan Thompson,[1] Richard Chen,[1] Jessica Thomaston,[2] William F. DeGrado,[2]* and Kathleen P. Howard[1]*

[1]Department of Chemistry and Biochemistry, Swarthmore College, Swarthmore, Pennsylvania 19081
[2]Department of Pharmaceutical Chemistry, University of California, San Francisco, San Francisco, California 94158

Abstract: The influenza A M2 protein is a 97-residue integral membrane protein involved in viral budding and proton conductance. Although crystal and NMR structures exist of truncated constructs of the protein, there is disagreement between models and only limited structural data are available for the full-length protein. Here, the structure of the C-terminal juxtamembrane region (sites 50–60) is investigated in the full-length M2 protein using site-directed spin-labeling electron paramagnetic resonance (EPR) spectroscopy in lipid bilayers. Sites 50–60 were chosen for study because this region has been shown to be critical to the role the M2 protein plays in viral budding. Continuous wave EPR spectra and power saturation data in the presence of paramagnetic membrane soluble oxygen are consistent with a membrane surface associated amphipathic helix. Comparison between data from the C-terminal juxtamembrane region in full-length M2 protein with data from a truncated M2 construct demonstrates that the line shapes and oxygen accessibilities are remarkably similar between the full-length and truncated form of the protein.

Keywords: full-length M2 protein; site-directed spin labeling; electron paramagnetic resonance; amphipathic helix; viral budding

## Introduction

The M2 protein is a 97-amino acid multifunctional protein that is assembled into a homotetramer and spans the viral membrane.[1] The proton channel activity of M2 has been extensively studied and is crucial for the uncoating of virions entrapped within endosomes.[2,3] M2 also plays a critical role in viral assembly and budding.[4–6] Influenza viruses are thought to utilize lipid raft domains in the plasma membrane of infected cells as sites of virus assembly and budding.[7] The C-terminal juxtamembrane region of M2 has been shown to be critical in generating membrane curvature[8] and facilitating viral budding.[9]
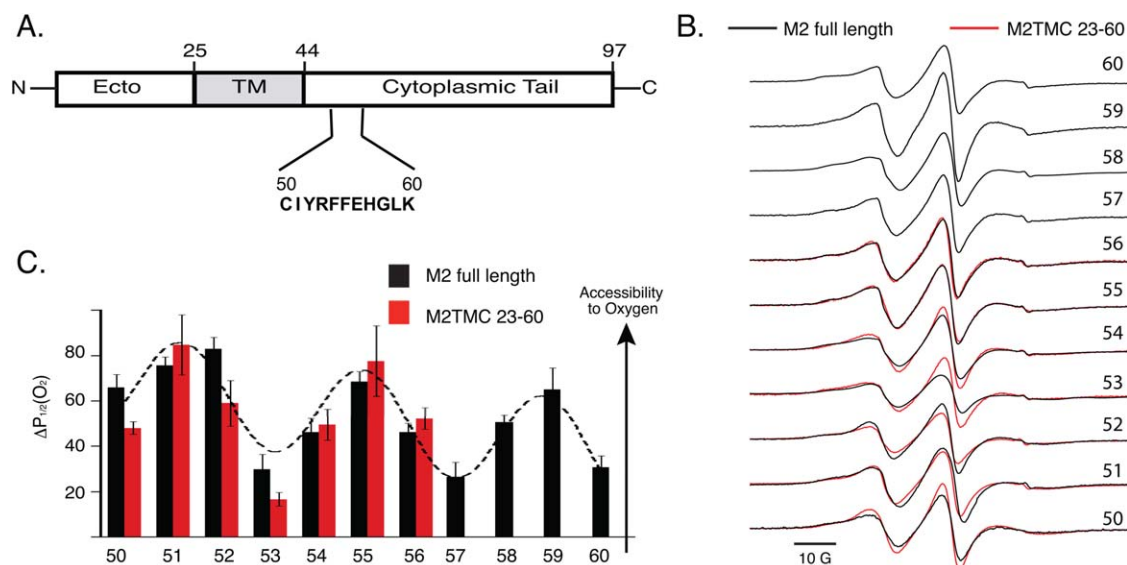
Figure 1. A. Domain structure of full-length M2 protein indicating the 11 sites (50–60) that were spin-labeled in this study. B. CW X-band EPR spectra of full-length M2 protein for sites 50–60 (black lines) and previously published spectra[10] for sites 50–56 in M2TMC (23–60) (red lines). C. Oxygen accessibilities for spin-labeled sites in full-length M2 protein (black bars) and previously published oxygen accessibilities[10] for sites 50–56 in M2TMC (23–60) (red bars). Error bars on the $\Delta P_{1/2}$ (O_2) bars are the 95% confidence intervals from the fits to the power saturation curves. M2TMC (23–60) SDSL-EPR data for sites 57–60 have not been published.

The domain structure of M2 protein is shown in Figure 1(A). Each monomer within the homotetramic protein consists of a small N-terminal ectodomain, a transmembrane domain, and a long cytoplasmic tail. A series of biophysical methods have probed the conformation and dynamics of the M2 protein.[8,11–14] Although preliminary structural studies on bacterially expressed full-length M2 protein have been published,[12,15] the majority of previously published papers have focused on chemically synthesized truncated M2 peptide constructs, M2TM (22–46) or the transmembrane domain plus approximately 14 proximal C-terminal residues, M2TMC (23–60).

In this article, we focus on the C-terminal juxtamembrane region of the full-length M2 protein due to its role in viral budding.[8,9] Previously published work on the C-terminal region in truncated versions of M2 protein from our lab[10,14] and others[11,13] have demonstrated this region forms an amphipathic helix. The question remains, however, whether this region has a similar secondary structure and membrane topology in the full-length M2 protein. To address this problem, we use the highly sensitive and information-rich method of site-directed spin label electron paramagnetic resonance spectroscopy (SDSL-EPR).[16] The advantage of SDSL-EPR is that it can be conducted at relatively low peptide to lipid ratios where crowding between proteins is unlikely to influence the dynamic properties of the protein. At the higher peptide to lipid ratios required for other methods such as solid-state nuclear magnetic resonance (NMR) spectroscopy, crowding between the densely packed M2 proteins might affect the

dynamic or even structural properties of the full-length protein. Here, we show that the structure and dynamics of the C-terminal juxtamembrane region are similar between the full-length and truncated forms of the protein.

Results and Discussion

EPR data for sites 50–60 in full-length M2 protein

Full-length M2 protein was expressed, purified, spin-labeled with (1-oxyl-2,2,5,5-tetramethyl-Δ3-pyrroline-3-methyl) methanethiosulfonate (MTSL) and reconstituted into 1-palmitoyl-2-oleoyl-sn-glycero-3-phosphocholine and 1-palmitoyl-2-oleoyl-sn-glycero-3-phospho-1-rac-glycerol (POPC:POPG) 4:1 lipid bilayer vesicles. This bilayer system was chosen because of its use in published M2 functional viral budding assays[17] and its use in previous SDSL-EPR work on the M2TMC (23–60) construct.[10,14] CW-X-band EPR spectra for the 11 single-site spin-labeled M2 proteins are shown in black in Figure 1(B). The breadth and shape of these EPR spectra are typical of spin-labels bound to a surface associated domain of a membrane-bound protein.[10,14]

Figure 1(C) shows the accessibility of sites 50–60 in the full-length protein to paramagnetic membrane soluble oxygen using power saturation methods (black bars). Molecular oxygen is a small hydrophobic species that generally partitions into lipid bilayers. Residue-by-residue patterns of measured accessibilities to O_2 represent a blueprint of a protein's secondary structure and topology with respect to the membrane.[16] Lipid accessibility data

for sites 50–60 show a sinusoidal variation with a periodicity of 3.6 typical for a surface absorbed α-helix (black dashed line). The lipid accessibilities match the physiochemical properties of individual amino acid side chains in the wild-type sequence. The most membrane-embedded residues (Ile 51, Phe 55, and Leu 59) are hydrophobic while the more water-exposed residues (Arg 53 and Lys 60) are hydrophilic.

Comparison of EPR data for full-length protein to a truncated construct M2TMC (23–60)

We have previously published SDSL-EPR data for sites 50–56 for a M2TMC (23–60) chemically synthesized truncation of the M2 protein.[10,14] The M2TMC (23–60) construct includes both the transmembrane domain and the first 14 residues of the C-terminal domain. An overlay of the CW X-band EPR line shapes for sites 50–56 in both the full-length (black lines) and truncated construct (red lines) are shown in Figure 1(B). The breadth of spectral line shapes between the full-length and truncated construct are similar. The spectra for sites 55 and 56 are indistinguishable. There are some differences in the amplitude of the central peak for sites 50–54. The addition of 37 residues past the end of the M2TMC (23–60) truncation undoubtedly modifies some of the dynamic properties of these sites in full-length M2.

In Figure 1(C), we compare the accessibility of paramagnetic membrane soluble oxygen to sites 50–56 in M2TMC 23–60 (red bars) to the same sites in full-length M2 protein (black bars). The oxygen accessibilities in the full-length version of M2 protein are strikingly similar to the accessibilities in the truncated version, with both sets of data consistent with a membrane surface associated amphipathic helix.

Conclusions

SDSL-EPR studies on the C-terminal juxtamembrane region in full-length M2 protein clearly demonstrate that this region forms an amphipathic helix that lies on the surface of the membrane. This biophysical evaluation is in complete accord with electrophysiological studies of full-length M2 in comparison to deletion mutants, which showed no appreciable differences in the proton channel activity and pharmacological inhibition between a number of constructs.[18] This work provides valuable new structural and membrane topology data for the full-length M2 protein, which has yet to be extensively characterized. Furthermore, the observation that the SDSL-EPR data collected for a truncated version of M2 is strikingly similar to full-length protein has implications for the use of truncated versions of M2 protein in studying how M2 promotes membrane curvature and viral budding.

Materials and Methods

Expression, spin labeling, and purification of M2 protein

The expression of the full-length M2 protein followed published protocols[19] with the following modifications. Eleven different M2 sequences were expressed with single site cysteine substitutions at residues 50–60 with native cysteines mutated to serine[20] so a spin label would attach specifically to one residue. Cysteine mutagenesis in this region is not detrimental to M2 function, with cysteine mutants in this region giving rise to channels with conductance and reversal potential properties very close to those observed for the wild-type channel.[10]

For each construct, a cell pellet from $1/4$ L of growth was suspended and vortexed in 9.5 mL of lysis buffer containing 50 mM Tris pH 8, 40 mM (octyl β-D-glucopyranoside) OG, 150 mM NaCl, 0.2 mg/mL DNase I, 0.25 mg/mL lysozyme, and 500 mM AEBSF. The mixture was sonicated on ice (20 min on 20% amplitude, 1 s on/1 s off pulse) and then centrifuged for 30 min at 15,000g. The supernatant was incubated with 1 mL Ni-NTA resin (GoldBio), 20 mM imidazole, and 20 mM β-mercaptoethanol and nutated at room temperature for 30 min. The column was washed successively with Wash I (50 mM Tris pH 8, 150 mM NaCl, 40 mM OG, 20% v/v glycerol), Wash II (50 mM Tris pH 8, 20 mM OG, 20% v/v glycerol), and then Wash III (50 mM Tris pH 8, 4 mM OG, 20% v/v glycerol, 20 mM imidazole). Tenfold molar excess of MTSL spin-label was dissolved in 16 μL of acetonitrile and then added to 1 mL of Wash III. The MTSL solution was added to the column and nutated at 4°C for 48 h. Spin-labeling buffer was then eluted from column. To facilitate the removal of free spin-label, 5 mL of Wash III was added to the column and the column was nutated at room temperature for 20 min. The column buffer was then eluted, and the column was washed with an additional 10 mL of Wash III. The His-tagged M2 protein was then eluted with 5 mL of elution buffer (50 mM Tris, 300 mM imidazole, 4 mM OG, and 20% v/v glycerol buffer). PD-10 desalting columns (GE Healthcare) using 50 mM Tris pH 8, 4 mM OG buffer were used to separate spin-labeled M2 protein from imidazole and excess free spin-label. Sodium dodecyl sulfate polyacrylamide gel electrophoresis (SDS-PAGE) was used to confirm purification of the protein.

Reconstitution of M2 protein into liposomes

Full-length M2 protein was reconstituted into lipid vesicles composed of 4:1 POPC:POPG. This bilayer system was chosen because of its use in published M2 functional fusion assays[17] and its use in previous SDSL-EPR work on the M2TMC (23–60) construct.[10,14] Chloroform solutions of POPC and POPG were combined in a 4:1 molar ratio. Chloroform was removed under a gentle stream of nitrogen and then the lipid films were

placed under high vacuum overnight. The lipid films were resuspended in 50 mM Tris pH 8, 100 mM KCl, 1 mM EDTA by alternately bath sonicating and vortexing the films. The lipid suspension was extruded 15 times through 20 μm filters using an Avanti Mini-Extruder. The lipids were solubilized with 50 mM Tris pH 8, 100 mM NaCl, 40 mM OG, to achieve a molar detergent to lipid ratio of 2.6. The lipid/detergent solution was then equilibrated for 30 min. Next, protein was added to achieve a protein to lipid molar concentration ratio of 1:500. A slurry of hydrophobic polystyrene beads (Bio-Beads SM-2, Bio-Rad) was made by adding buffer (50 mM Tris pH 8, 100 mM NaCl) dropwise to the beads until they were hydrated. The Bio-Bead slurry was stirred slowly and degassed under vacuum for 1 h. While the proteoliposomes were gently nutated at 4°C, five different 50 μL aliquots of a Bio-Bead slurry were added at 15 min intervals. A final 200 μL aliquot of Bio-Beads was added to the proteoliposome solution and nutated overnight at 4°C. After the Bio-Beads were removed, the proteoliposome solution was then concentrated to a spin-labeled protein concentration of approximately 100 μM using Amicon Ultra-0.5 Centrifugal Filter Devices at 13,000g.

EPR spectroscopy

Continuous wave (CW) EPR spectra were recorded at room temperature on an X-band Bruker EMX spectrometer equipped with an ER4123D resonator. Samples used for analysis of spectral line shapes were placed in glass capillary tubes and EPR spectra were acquired using 2 mW incident microwave power, 1 G field modulation amplitude at 100 kHz, and 150 G sweep width. For comparison of line shapes, each spectrum was double integrated and normalized to the same number of spins.

For power saturation measurements, samples were collected in gas-permeable TPX capillary tubes. Power saturation data were obtained under two sets of conditions, equilibrated with nitrogen gas and equilibrated with ambient air. For experiments with low accessibility to fast relaxing paramagnetic reagents, EPR spectra were measured at eight power levels. For experiments with high accessibility to paramagnetic reagents, 16 power levels were studied as the saturation effect was sometimes significantly mitigated and thus more data points were required to achieve a good fit. Data were analyzed and $\Delta P_{1/2}$ parameters reflecting side chain accessibility to paramagnetic reagents were determined as described previously.[10]

References

1. Pinto LH, Lamb RA (2006) The M2 proton channels of influenza A and B viruses. J Biol Chem 281:8997–9000.
2. Stauffer S, Feng Y, Nebioglu F, Heilig R, Picotti P, Helenius A (2014) Stepwise priming by acidic pH and a high K+ concentration is required for efficient uncoating of influenza A virus cores after penetration. J Virol 88:13029–13046.
3. Wang J, Qiu JX, Soto C, DeGrado WF (2011) Structural and dynamic mechanisms for the function and inhibition of the M2 proton channel from influenza A virus. Curr Opin Struct Biol 21:68–80.
4. Rossman JS, Jing XH, Leser GP, Balannik V, Pinto LH, Lamb RA (2010) Influenza virus M2 ion channel protein is necessary for filamentous virion formation. J Virol 84:5078–5088.
5. Rossman JS, Lamb RA (2011) Influenza virus assembly and budding. Virology 85:229–236.
6. Stewart SM, Pekosz A (2011) Mutations in the membrane-proximal region of the influenza A virus M2 protein cytoplasmic tail have modest effects on virus replication. J Virol 85:12179–12187.
7. Rossman JS, Lamb RA (2013) Viral membrane scission. Annu Rev Cell Dev Biol 29:551–569.
8. Schmidt NW, Mishra A, Wang J, DeGrado WF, Wong GCL (2013) Influenza virus A M2 protein generates negative Gaussian membrane curvature necessary for budding and scission. J Am Chem Soc 135:13710–13719.
9. Roberts KL, Leser GP, Ma CL, Lamb RA (2013) The amphipathic helix of influenza A virus M2 protein is required for filamentous bud formation and scission of filamentous and spherical particles. J Virol 87:9973–9982.
10. Nguyen PA, Soto CS, Polishchuk A, Caputo GA, Tatko CD, Ma CL, Ohigashi Y, Pinto LH, DeGrado WF, Howard KP (2008) pH-induced conformational change of the influenza M2 protein C-terminal domain. Biochemistry 47:9934–9936.
11. Claridge JK, Aittoniemi J, Cooper DM, Schnell JR (2013) Isotropic bicelles stabilize the juxtamembrane region of the influenza M2 protein for solution NMR studies. Biochemistry 52:8420–8429.
12. Liao SY, Fritzsching KJ, Hong M (2013) Conformational analysis of the full-length M2 protein of the influenza A virus using solid-state NMR. Protein Sci 22:1623–1638.
13. Cross TA, Ekanayake V, Paulino J, Wright A (2014) Solid state NMR: the essential technology for helical membrane protein structural characterization. J Mag Res 239:100–109.
14. Thomaston JL, Nguyen PA, Brown EC, Upshur MA, Wang J, Degrado WF, Howard KP (2013) Detection of drug-induced conformational change of a transmembrane protein in lipid bilayers using site-directed spin labeling. Protein Sci 22:65–73.
15. Tian C, Gao PF, Pinto LH, Lamb RA, Cross TA (2003) Initial structural and dynamic characterization of the M2 protein transmembrane and amphipathic helices in lipid bilayers. Protein Sci 12:2597–2605.
16. Klug CS, Feix JB (2008) Methods and applications of site-directed spin Labeling EPR Spectroscopy. Biophysical tools for biologists: vol 1 in vitro techniques. San Diego, CA: Elsevier Academic Press Inc., pp 617–658.
17. Rossman JS, Jing XH, Leser GP, Lamb RA (2010) Influenza virus M2 protein mediates ESCRT-independent membrane scission. Cell 142:902–913.
18. Ma C, Polishchuk AL, Ohigashi Y, Stouffer AL, Schon A, Magavern E, Jing X, Lear JD, Freire E, Lamb RA, DeGrado WF, Pinto LH (2009) Identification of the functional core of the influenza A virus A/M2 proton-selective ion channel. Proc Natl Acad Sci USA 106:12283–12288.
19. Leiding T, Wang J, Martinsson J, DeGrado W, Arskold S (2010) Proton and cation transport activity of the M2 proton channel from influenza A virus. Proc Natl Acad Sci USA 107:15409–15414.
20. Holsinger LJ, Shaughnessy MA, Micko A, Pinto LH, Lamb RA (1995) Analysis of the posttranslational modifications of the influenza virus M2 protein. J Virol 69:1219–1225.